VORTEX SHEDDING FROM TWO SURFACE-MOUNTED CUBES IN TANDEM

Robert J. Martinuzzi and Brian Havel
Advanced Fluid Mechanics Research Group
Department of Mechanical and Materials Engineering
Faculty of Engineering, University of Western Ontario
London, Ontario, N6A 5B9, Canada

ABSTRACT

Periodic vortex shedding from two surface-mounted cubes, of height H, in tandem arrangement placed in a thin boundary layer is investigated for a spacing 2H using phase-averaged laser Doppler velocimetry. Tests were conducted for a Reynolds number of 22000, based on H and the freestream velocity, and an approximately 0.07H thick laminar boundary layer. For obstacle separations between 1.5H and 2.5H, the shedding frequency scales linearly with the obstacle spacing. In this lock-in regime, periodic shedding is triggered by the interference between a vertical flow stream along the front face of the downstream obstacle and the vortex in the inter-obstacle gap. The mechanism is different from that observed for two-dimensional geometries and helps explain why lock-in cannot be observed for square cylinders in tandem arrangement. The shedding event is accompanied by an abrupt increase in the random contribution to the turbulence field.

INTRODUCTION

The flow around multiple bluff bodies has been extensively studied due to its practical significance in many engineering applications, for exampling, in determining dynamic loading on neighboring structures or the influence on heat transfer. An important mechanism for flow-structure interaction arises from the coupled interference between the obstacles on the vortex formation and shedding process.

Rockwell (1998) provides an encompassing review of the studies conducted for two-dimensional bluff bodies. When an obstacle undergoes forced periodic oscillations, the shedding frequency can lock on to the frequency of obstacle oscillations if the two are not too different. Gaydon and Rockwell (1999) have shown that, for a fixed obstacles, incident vortices can dramatically shorten the formation length in the cylinder wake and modify the vortex shedding frequency and can also result in lock on. Similarly, when two cylinders are placed in tandem in a uniform stream, the shedding frequency from the second obstacle can lock on to that of the first obstacle over a critical obstacle spacing range (cf. Zdravkovich, 1977; Albrecht et al., 1988). As the spacing between the obstacles is changed, up to four regimes have been identified for both circular (Zdravkovich, 1977) and square cylinders (Hangan and Vickery, 1999) in tandem arrangement. For very small obstacle separation, the flow is similar to that for a single bluff body. For intermediate separations, there is a region of bistable flow, for which two non-harmonic frequencies are reported. This behaviour is similar to that reported by Okajima (1982) for large aspect ratio rectangular bluff bodies. For larger separations, the shedding frequency from the second obstacle locks on to that of the first. For very large separations, the obstacles shed independently.

Three-dimensional geometries have received much less attention, possibly because these often occur deep in boundary layers and periodic vortex shedding is suppressed. However, if the boundary layer thickness is less than approximately 70% of the body height, vortex shedding is observed (cf. Castro and Robins, 1977; Sakamoto and Haniu, 1988). For surface-mounted rectangular bluff bodies in tandem arrangement, bistable, lock-on and large separation regimes similar to those for the two-dimensional geometries have been reported by Sakamoto and Haniu (1988) and Havel et al. (2001). However, Martinuzzi and Havel (2000) have shown that the three-dimensional geometry shows a critical range, between the intermittent and the bistable regimes, where the shedding frequency scales linearly with the obstacle spacing. Effectively, the shedding frequency locks into the cavity flow.

In this work, the flow in the cavity between two surface-mounted cubes in the lock-in regime is investigated for the purpose of understanding why the shedding frequency scales with the obstacle gap and why a similar regime is not observed for two-dimensional obstacles in tandem arrangement. The cubes are mounted two obstacle heights apart and placed in a thin boundary layer. Based on surface pressure and laser Doppler velocimetry measurements, mean and phase-averaged representations of the flow field are used to investigate the shedding process greater detail and discuss some aspects of the turbulence field.

EXPERIMENTAL DETAILS

The flow was produced in an open, suction-type wind tunnel with a honeycomb and fine grid at the inlet. Air flowed through a 4:1 contraction into a 0.46 × 0.46 m^2 test section. The inlet profile was uniform within 1% of the free stream velocity, U_∞ = 8.8 m/s, and the free stream turbulence intensity was less than 1.5% as measured with a hot-wire anemometer. The experimental set-up and nomenclature is shown schematically in Fig. 1. Two cubes of dimension H = 0.04 m were mounted on a thin (3mm) flat plate along the streamwise line of symmetry of the test-section at a distance of 2H from the leading edge. A plate end-flap was adjusted to control separation at the plate leading edge and maintain a thin boundary layer.The Reynolds number based on cube height, H, and free-stream velocity U_∞ was 22000. The on-coming boundary layer was laminar and matched the Blasius profile. At the mounting point of the first cube, x = 2.5H, the boundary layer thickness was $\delta/H \approx 0.07$.

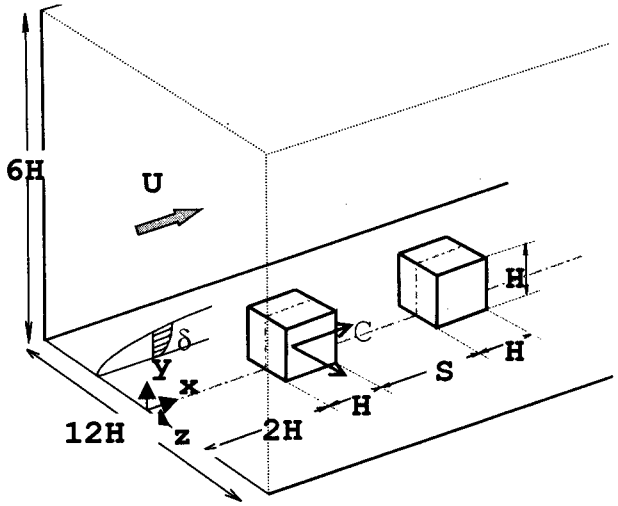

Figure 1: Set-up schematic and nomenclature.

Surface pressure measurements were made at several locations on the plate and cube surfaces. The pressure taps were 0.7mm in diameter. The reference was taken as the free-stream static pressure from the pitot static tube.. The frequency response of the system (pressure tap, tubing, and sensor) was flat to 200 Hz. The transducer resolution was ±0.5Pa and data was sampled at 2kHz.

Velocity data was acquired with a two-component LDV. The optical setup consisted of a 0.453 m focal length lens with a 2.6 × beam expander resulting in a measurement volume of diameter 46μm and length 340μm. The LDV processor was a two channel TSI IFA 655 correlator operated in single-measurement-per-burst (SMB) mode. The coincidence window between the two velocity channels was set to 200μs, based on preliminary measurements at several locations showing the shear stress coefficient was insensitive to the coincidence window setting in the range 50μs to 500μs. A frequency shift of 5 MHz was applied to both measurement channels to eliminate directional ambiguity.

The flow was seeded at the upstream of the honeycomb with an atomized 10:1 water-glycerol mixture. The particle number mean diameter was 4μm with 90% of the particles being less than 8μm. Following Rudoff and Bachalo (1991), these particles are expected to follow the flow.

The phase-averaged velocity field was analysed subject to the triple decomposition:

$$U^*_i = u_i + u_{ci} + u'_i$$

where: U^*_i is the instantaneous velocity, u_i is the local long-time mean, u_{ci} is the fluctuating coherent (phase-average) and u'_i is the turbulent (incoherent) contribution. The subscript i indicates the velocity component. The common reference event for all data points was taken as the peak pressure during each shedding period measured on the side face of the upstream cube. Individual cycle periods were determined from the peak-to-peak time differences. The velocity data were then redistributed over 20 equally spaced bins to reconstruct a phase-averaged cycle.

Mean and phase-averaged measurements of the three velocity components were made in ten normal and horizontal planes, each containing between 300 and 1100 measurement points. Typical data rates, N, ranged from 200Hz, in the base regions, to 5kHz in the shear layers. The average shedding frequency was 23Hz. At each point, data was collected for at least 50,000 LDV-events or 1000 shedding cycles. Only two perpendicular velocity components could be recorded simultaneously. It was thus necessary to measure each plane twice to obtain the three velocity components: u (streamwise), v (vertical), and w (spanwise). The redundant data, usually the streamwise component, were used to verify repeatability and uncertainty estimates.

The Taylor micro time scale, T_λ, was estimated at several stations in the flow field from the autocorrelation function of the streamwise velocity. The effective data density, NT_λ, was greater than 5 everywhere, which according to Edwards (1987) ensures very low velocity bias when using transit-time weighting. The velocity uncertainty was estimated to be 1% in the mean and 5% for phase-averaged statistics in a 95% confidence interval (cf. Benedict and Gould, 1996). These estimates were verified using the redundant u-velocity measurements. The measurement volume was positioned using a three-axis traversing platform accurate to 10μm/m.

RESULTS

For low aspect ratio, square cross-section, surface mounted obstacles arranged in tandem, Sakamoto and Haniu (1988), for obstacles 3H high, and Martinuzzi and Havel (2000), for cubes, identified four distinct shedding regimes have been identified based on the obstacle spacing, S. The average vortex shedding frequency, f, measured in downstream of two cubes is shown in Fig. 2 as a function of S/H expressed in terms of the non-dimensional Strouhal number based H, $St_H = fH/U_\infty$, and the spacing, $St_S = fS/U_\infty$. For the intermittent regime, S/H < 1.5, vortex shedding is interrupted by periods of random fluctuations. For the lock-in regime, 1.5 < S/H < 2.5, the vortex shedding is continuous and the frequency scales linearly with S. There exists a bistable regime, for which two non-harmonic shedding frequencies can be recorded simultaneously (4<S/H<6 in Fig. 2). For larger obstacle separations, the shedding frequency asymptotically approaches the value for the isolated cubes.

For the analogous, two-dimensional geometry, *i.e.* square cross-section cylinders in tandem in a uniform stream, a lock-in regime is not observed and there is an abrupt transition from continuous to irregular vortex shedding occurring at S/H≈2 (cf. Havel et al., 2001).

The differences in flow behavior can be conveniently summarized from the changes in the drag coefficient, C_D based on the frontal area and free-stream velocity, measured on the two obstacles as a function of spacing as shown in Fig. 3. For the two-dimensional geometry, C_D for both obstacles shows an abrupt drop at S/H≈2. This spacing coincides with the sudden transition from intermittent to continuously periodic shedding. For larger spacing, C_D for the first obstacle is approximately that for the single body in a uniform stream (C_D≈2.1). The lower C_D-value for the second body for S/H>2 results from the reduced flow speed in the wake of the upstream obstacle.

In contrast, for the three-dimensional geometries, the drag coefficient varies smoothly from the intermittent to the continuous shedding regimes. For the upstream obstacle, C_D initially decreases as S/H increases, reaching a minimum approximately at the end of the lock-in regime. For the downstream obstacle, the end of lock-in is marked by an inflection in the C_D vs. S/H curve.

To elucidate why a lock-in regime is observed for three, but not two-dimensional, tandem geometries requires a detailed investigation of the velocity field. First, the mean velocity field will be described to highlight some of the marking features in the lock-in regime. Subsequently, the shedding mechanism will be discussed in light of the velocity fields at different phases of the shedding cycle.

The flow field for two cubes in tandem at a spacing of S/H=2 is representative for the lock-in regime (1.5<S/H<2.5). The mean velocity components in the plane of symmetry, z/H=0, and in the horizontal plane, y/H=0.375, are shown as vectors along with selected sectional streamtraces in Fig. 4. A similar flow topology is observed in the horizontal planes 0.05< y/H<0.75.

From Fig. 4a, the dividing streamline in the separated shear layer, originating at the upstream cube leading edge, impinges at the leading edge corner at the top of the downstream cube. There is a strong vertical flow directed towards the wall along the front face. On the top face, the flow is attached. This flow pattern is similar through the lock-in regime. The flow patterns for S/H outside the lock-in regime has been investigated by Martinuzzi and Havel (2000). For S/H<1.5, the dividing streamline attaches on the top face of the downstream cube. Thus the cube interferes directly with the vortex formation process, resulting in irregular shedding of vortices. For S/H larger than for lock-in, the separated shear layer attaches upstream of the second cube, forming a new horseshoe vortex at its base. A stagnation point appears on the front face of this cube and the strong downward vertical stream is no longer observed. This change results in higher pressures on the front face of the cube, which are observed as an increase in the drag coefficient. The flow patterns around the upstream cube, however, change little and it is thus not surprising that the drag coefficient is insensitive to S/H.

In the horizontal plane, Fig. 4b, the large, counter-rotating recirculation vortices between the obstacles, with foci

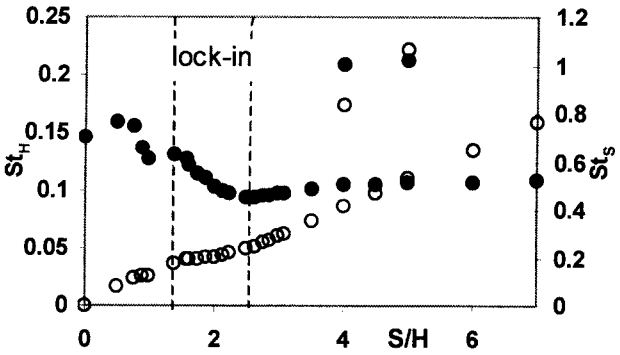

Figure 2: Shedding frequency in terms of the non-dimensional Strouhal numbers based on H, St_H (closed symbols), and S, St_S (open symbols) as s function of the gap size, S.

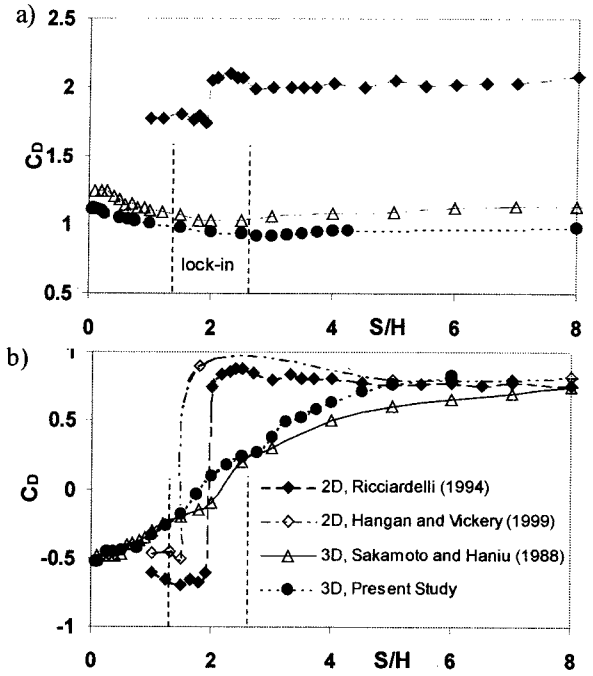

Figure 3: Drag coefficient, C_D, *vs* S/H for a) upstream and b) downstream obstacles in tandem arrangements of two square-cylinders, tall prism and cubes.

labelled V1 and V2, and the two saddle points, S1 and S2, are the principal topological features of interest. As is discussed below, circulation is periodically advected downstream from these vortices, in alternating fashion, to form a vortex street in the wake. The two saddle points mark the maximum mean downstream extent of these vortices. These form due to the interference between the recirculation vortices and the vertical flow along the windward face of the downstream obstacle. This three-dimensional effect cannot exist in the case of the tandem square cylinder geometry. Also note that the flow along the side faces of the downstream obstacle is attached.

For S/H larger than lock-in, the mean flow topology resembles that for a single square cylinder in a uniform stream. The separated shear layer from the top of the upstream obstacle impinges upstream of the second obstacle. The saddle points S1 and S2 merge to form a single saddle point along the plane of symmetry, which marks the end of

the formation region. The flow separates on the side faces of the downstream obstacle and it is observed that the shedding of vortices from the base of the downstream obstacle are no longer synchronized with those from the upstream obstacle, giving rise to a second, non-harmonic, spectral peak.

In the following section, it is proposed that the triggering mechanism for vortex shedding in the lock-in regime is three-dimensional in nature and thus fundamentally different from the classical, two-dimensional model. The latter is comprehensively discussed by Williamson (1996) and is here only briefly summarized.

Consider the vortex formation process on a cylinder placed in a uniform flow from left to right. The shedding cycle,

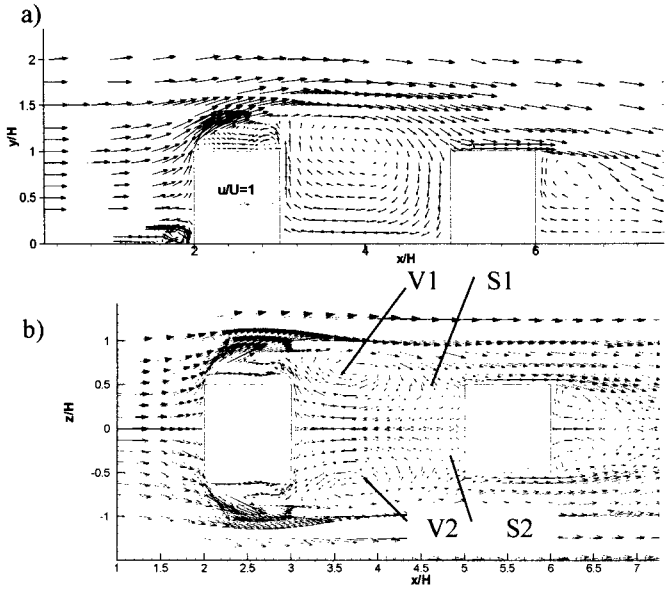

Figure 4: Mean flow representation in vector form for tandem cubes of spacing S/H=2: a) plane z/H=0; b) plane y/H=0.375.

arbitrarily chosen to start with the formation of a vortex on the upper face, can be described as follows. The flow separates and reattaches on this face giving rise to a clockwise rotating recirculation vortex. This vortex grows along the leeward face, fed by circulation generated at the separation point on the upper face and entrained into the base region. The vortex grows until it covers the entire leeward face, at which point the separation streamline interferes with the opposing shear layer from the lower face. As a result, a saddle point forms along the lower sehar layer downstream of the obstacle, which cuts off the flow of circulation from the lower separation point to the counter-clockwise rotating vortex in the base region. This vortex subsequently sheds.

The bottom shear layer now reattaches along the lower face of the cylinder and a counter-clockwise recirculation vortex begins to grow upward along the leeward face. This new vortex displaces the clockwise vortex into the base region. The clockwise vortex is still fed by circulation from the upper shear layer and thus continues to grow as well. However, the counter-clockwise vortex eventually extends over the entire leeward face and interferes with upper shear layer, thereby cutting off the flow of circulation to the clockwise vortex, which sheds. The upper shear layer reattaches on the upper face and the cycle is repeated.

The shedding process for the tandem, surface-mounted cube geometry is shown in Fig. 5 and 6 for selected phases of the shedding cycle. The phase averaged streamwise, u, and spanwise, w, velocity components in the plane y/H=0.25 are shown as vectors in Fig. 5, while the contours represent the vertical velocity component, v, in Fig. 6. The flow field topology is found to be similar for all horizontal planes $0.05<y/H<0.75$. However, it is observed that the location of the nodes for each phase is slightly different, indicating that the rotation axis of the flow structures is slightly tilted relative to a vertical axis. Note that the results are presented in an absolute frame of reference and the sectional streamtraces are included as visual aids.

Significant differences between the two- and three-dimensional shedding processes are seen by inspection of Fig. 5. Unlike the two-dimensional case, well-developed recirculation vortices are observed in the base region of the upstream obstacle. Phase 1 (ϕ=0°, Fig. 5a) is arbitrarily defined at the phase of the shedding cycle immediately after the upper vortex has shed. A saddle point, S1, is located directly downstream of the upper base vortex, V1. Note that there is a strong vertical down flow along the front face of the downstream cube (Fig. 6a). The dividing streamline along the lower shear layer impinges on the cube corner. The flow is attached along the side of the cube and circulation is fed to the counter-clockwise base vortex V2, which continues to grow as shown in Fig. 5b, ϕ=54°. At the this phase, the centre of the region of vertical flow, shown in Fig. 6b, reaches its maximum upward location and the spanwise flow along the front face is directed towards the top leading edge. Both V1 and V2 continue to grow.

The core of the vortex V2 and the saddle point S1move downstream until the location of S1 coincides with the upper leading edge corner of the downstream cube. There is a rapid switch in the direction of the spanwise flow, within a shedding phase difference of ϕ=20°, towards the lower leading edge and the vertical stream moves towards the lower leading edge, as in Fig. 6c for ϕ=162°, to interfere with the bottom shear layer flow causing the appearance of a saddle point, and a counter-clockwise vortex sheds. At this phase of the shedding cycle, the dividing streamline along the upper shear layer now impinges on the leading corner of the downstream cube, while the lower shear layer no longer attaches on the obstacle lower face. In Fig. 5c, ϕ=162°, the saddle point S2 is clearly visible, the vortex V2 is reduced in size and the top vortex, V1, penetrates deeply into the inter-obstacle cavity. The half-cycle is then repeated, but 180° out of phase, to lead to the shedding of V1.

Contrary to the two-dimensional case, however, the vortex V1 is still contained to the upper half of the flow plane. In the classical model, the top vortex grows in the base region and eventually extends across the leeward face to interfere with the bottom shear layer, thereby cutting off the flow of circulation to the bottom vortex and causing it to shed.

For the present three-dimensional case, however, it is the stream of strong vertical flow along the face of the second cube which moves towards the bottom leading edge. The vertical stream thus appears to have split the vortex V2. Part

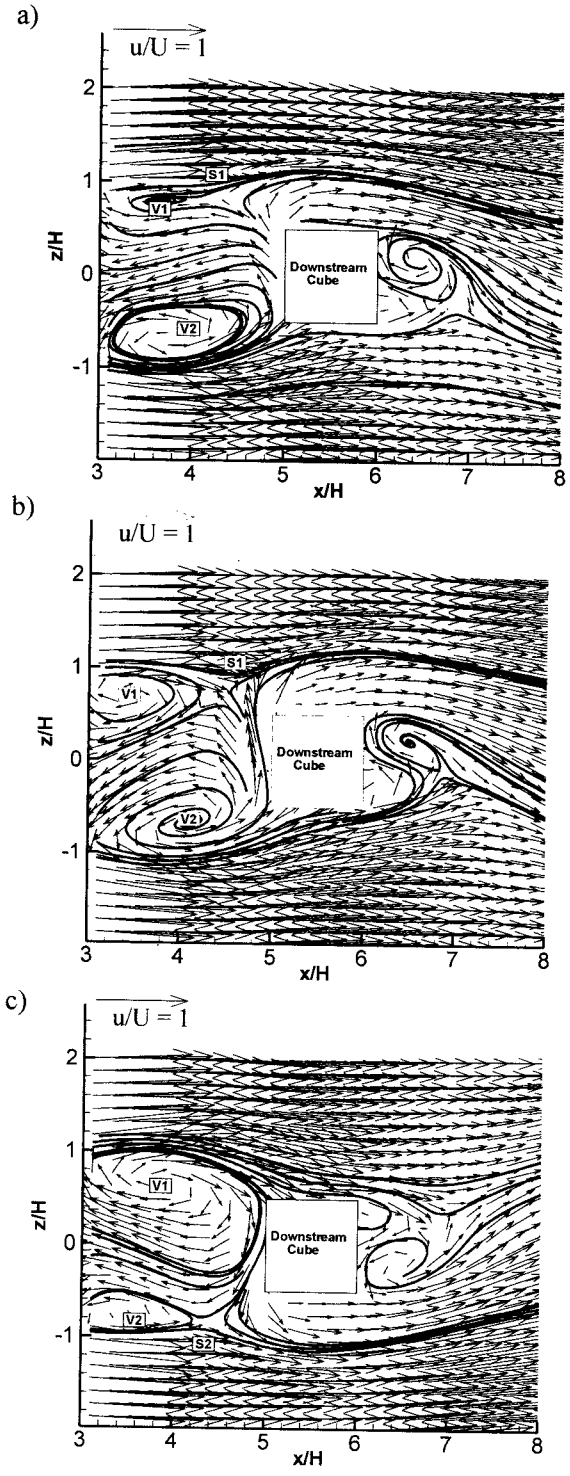

Figure 5: Phase-averaged vector representation of the u-w velocity components in the plane y/H=0.25 for phases a) ϕ=0°; b) ϕ=54° and c) ϕ=162°

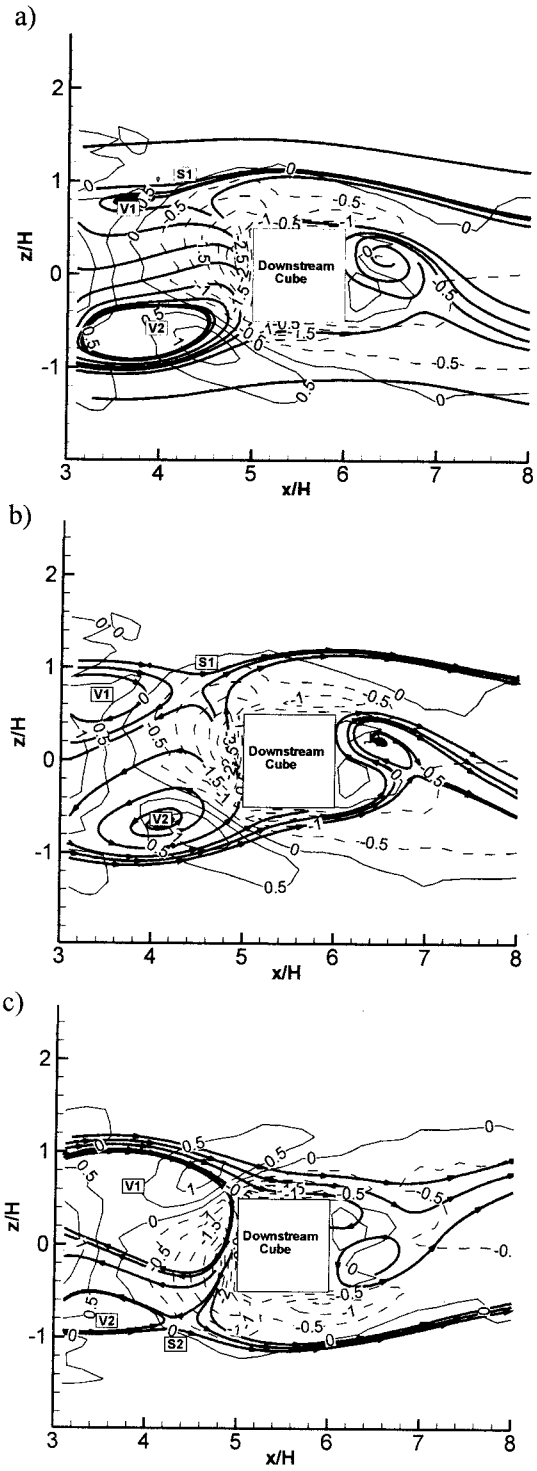

Figure 6: Phase-averaged contour representation of the vertical, v, velocity component in the plane y/H=0.25 for phases a) ϕ=0°; b) ϕ=54° and c) ϕ=162°

of this vortex is shed, while the remainder begins to grow again, fed by the circulation from the bottom shear layer.

DISCUSSION

The relative shift in the spanwise location of the vertical stream serves to trigger shedding and is accompanied by a large increase in the random contribution to the turbulence kinetic energy, <k>. In Fig. 7a, the <k> distribution is shown for the phase ϕ=54° (see Fig. 5b). An absolute maximum is observed around the location of the saddle point S1. Part of the turbulence is convected downstream with the shed vortex, but a significant amount is convected to the opposite side of the second cube. In Fig. 7b, the random contribution to the production term is shown for the same phase. Again a maximum occurs near S1. However, it is noted that the production term is otherwise small outside the

shear layers, indicating that the high levels of <k> found elsewhere are mainly due to advection. Furthermore, the downward vertical stream results in relatively little shear (*i.e.* little vorticity is associated with it), except in the region of interference with the side shear layer. These observations suggest that the effects of the stream are highly localized.

CONCLUDING REMARKS

In the two-dimensional case, shedding is triggered by the interference between the forming vortex and the opposite shear layer. For three-dimensional geometries in the lock-in regime, the vortex sheds as a result of the interference between the vertical stream along the front face of the downstream obstacle and the side shear layers. The opposite vortex induces the spanwise flow across the face of the downstream cube, which provides the opposing shear layer coupling necessary for stable, periodic shedding. It thus appears reasonable to expect that the shedding frequency will scale linearly with the obstacle spacing, since the shedding is triggered by the vertical stream and that the location of this stream is determined by the location of the second obstacle.

The existence of the vertical stream along the downstream obstacle windward face is necessary for lock-in to occur. Thus, when the obstacle spacing is increased sufficiently, the top shear layer attaches upstream of the downstream obstacle, eliminating the vertical stream. The vertical stream is a three-dimensional effect and does not exist for two-dimensional tandem arrangements which may explain why lock-in has not been observed in these cases.

REFERENCES

Albrecht, T., Barnes, F.H., Baxendale, A.J. and Grant, I., 1988, "Vortex Shedding from Two Cylinders in Tandem," *J. Wind Eng. & Ind. Aero.*, 28: 201-208.

Benedict, L.J. and Gould, R.D., 1996, "Towards Better Uncertainty for Turbulent Statistics," *Exp. in Fluids,* 107:161-164.

Castro, I.P. and Robins, A.G., 1977,"The flow around a surface-mounted cube in uniform and turbulent streams," *J. Fluid Mech.*, 79Z: 307-335.

Edwards, R.V., 1987, "Report of the Special Panel on Statistical Particle Bias Problems in Laser Anemometry," *Trns. ASME, J. Fluids Eng.* 109:89-93.

Gaydon, M. and Rockwell, D., 1999, "Vortices incident upon oscillating cylinder: Flow structure and loading," *J. Fluids & Struc.*, 13: 709-722.

Hangan, H. and Vickery, B.J., 1999,"Buffeting of 2D (sharp-edged) bluff bodies," *J. Wind Eng. & Ind. Aero.*, 82: 173-187.

Havel, B., Hangan, H. and Martinuzzi, R., 2001, "Buffeting for 2D and 3D sharp-edged bluff bodies," *J. Wind Eng. & Ind. Aero.*, 89:1369-1381.

Martinuzzi, R. and Havel, B., 2000, "Turbulent flow around two interfering surface-mounted cubic obstacles in tandem arrangement," *Trns. ASME, J. Fluids Eng.* 122:24-31

Okajima, A., 1982,"Strouhal numbers of rectangular cylinders," *J. Fluid Mech.*, 123: 379-398.

Ricciardelli, F., 1994, *Aerodynamics of a pair of square cylinders,* M.E.Sc. Thesis, The University of Western Ontario, London, Ontario, Canada.

Rockwell, D., 1998, "Vortex Body Interactions," *Ann. Rev. in Fluid Mech.*, 30: 199-229.

Rudoff, R.C. and Bachalo, W.D., 1991, "Seed Particle Response and Size Characterization in High Speed Flows," *Proc. ASME Fluids Eng. Conf., Symp. On Laser Anem., Adv. and Appl.*, 2:443-447.

Sakamoto, H. and Haniu, H., 1988,"Aerodynamic forces acting on two square prisms placed vertically in a turbulent boundary layer," *J. Wind Eng. & Ind. Aero.*, 31:41-66.

Williamson, C.H.K., 1996, "Vortex Dynamics in the Cylinder Wake," *Ann. Rev. in Fluid Mech.*, 28: 477-539 *Ann. Rev. in Fluid Mech.*, 30: 199-229.

Zdravkovich, M.M., 1977,"Review of flow interference between two circular cylinders in various arrangements," *Trns. ASME, J. Fluids Eng.*, 99: 618-633.

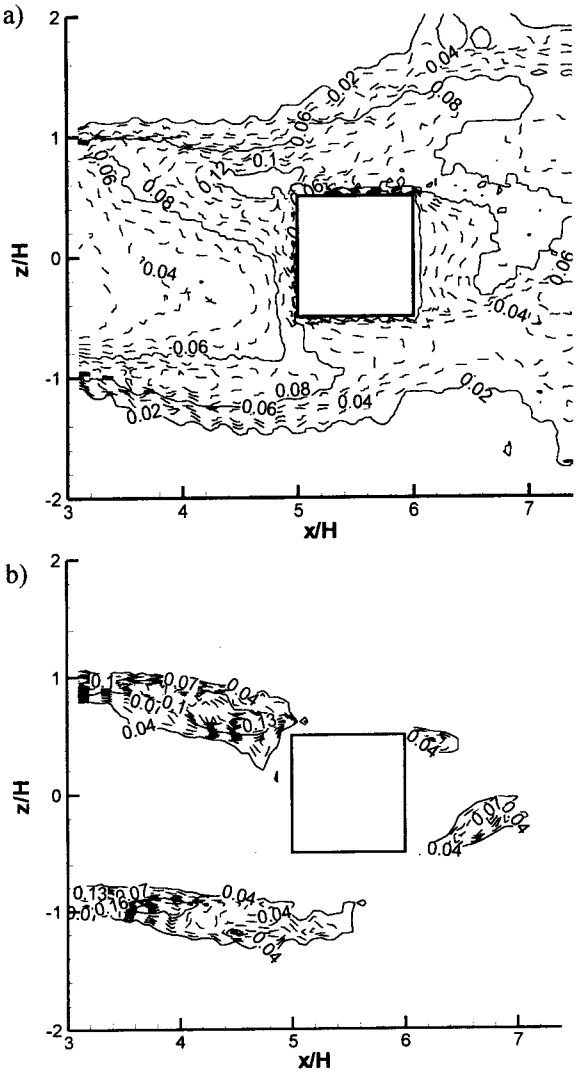

Figure 7: Contours of the normalized random contributions: a) <k> and b) production terms for shedding phase ϕ=54°